

# Isoscalar Monopole Strength in $^{100}\text{Mo}$ : an Indicator for Static Triaxial Deformation in The Ground State

Yue Shi (石跃)<sup>1,\*</sup> and P. D. Stevenson<sup>2,†</sup>

<sup>1</sup>*Department of Physics, Harbin Institute of Technology, Harbin 150001, People's Republic of China*

<sup>2</sup>*Department of Physics, University of Surrey, Guildford, GU2 7XH, United Kingdom*

**Background** The giant isoscalar monopole (ISM) resonances can be connected with the incompressibility of uniform nuclear matter. Experimental and theoretical studies suggest that the structural effect may present in the ISM strengths. Recently observed ISM strengths in  $^{100}\text{Mo}$  show a multiple peak structure, which may indicate an onset of static triaxial deformations in the ground state of this nucleus.

**Purpose** We intend to perform a microscopic study of the ISM strength of  $^{100}\text{Mo}$  and study if the observed features are due to a triaxially deformed ground state.

**Methods** We perform deformation constraint symmetry-unrestricted 3D time-dependent density functional theory (TDDFT) calculations for the ISM mode in  $^{100}\text{Mo}$ . Monopole moment as a function of time is obtained by time propagating states based on deformations. A Fourier transform is then performed on the obtained response functions of the monopole and quadrupole moments. The resulted ISM strength functions are compared with experimental data.

**Results** The calculated results using four different energy-density functionals show that a  $\beta_2$  value of 0.25 give a two-peak structure of the strength function. With increasing  $\gamma$  from  $10^\circ$  to  $30^\circ$  results in the lower peak to split into two, making the general shape of the strength functions closer to the data.

**Conclusions** Our microscopic TDDFT + BCS analyses suggest that the  $^{100}\text{Mo}$  is triaxially deformed in the ground state. The calculated isoscalar  $Q_{20}$  and  $Q_{22}$  strength functions peak at lower energies. The coupling of these two modes with the ISM mode is the reason for the three-peak/plateau structure in the strength function of  $^{100}\text{Mo}$ .

PACS numbers:

## I. INTRODUCTION

Recent years have seen renewed interest in the compression-mode resonances, such as the isoscalar giant resonances in nuclear physics [3]. From the resonance it is possible to extract the incompressibility of the uniform nuclear matter, which is an important parameter of the equation of state.

In various density functional theories, the incompressibility parameter naturally arises as soon as the model parameters are determined<sup>1</sup>. Consequently, it is customary to take an energy density functional that successfully describes properties of finite nuclei and examine its performance when applied to the description of the isoscalar giant monopole resonance. If the theory can simultaneously account for the ground-state data as well as the observed resonance energies, then its incompressibility is considered reliable.

Although progress has been made [4], some issues remain. For example, most EDFs systematically overestimate the isoscalar giant monopole resonance energies of tin isotopes [5]. This is curious because the same theories can reproduce the ground state observables as well as the resonance energies in other nuclei, such as  $^{90}\text{Zr}$  and

$^{208}\text{Pb}$  [6]. This suggests that the structural information becomes important in describing the isoscalar monopole (ISM) mode and the current theories seem to be lacking. To have a better model and hence an accurate incompressibility parameter, it is desirable to expand the knowledge of the ISM vibration in other nuclei.

Recently, the ISM mode were observed systematically and the associated strengths were extracted for  $^{90}\text{Zr}$ ,  $^{92,94,96,98,100}\text{Mo}$  nuclei [1, 2]. Focusing on the Mo isotopes, for  $^{92,94,96,98}\text{Mo}$ , the observed strengths as a function of excitation energy show generic single peaks around  $16 < E < 17$  MeV. From  $^{94}\text{Mo}$ , a lower-energy shoulder starts to emerge near  $E = 13$  MeV and becomes more pronounced in  $^{96,98}\text{Mo}$ . For  $^{100}\text{Mo}$ , the structure of the strength function shows a multi-peak feature.

While the strengths in the lighter Mo isotopes seem to be due to a spherical or weak deformation, the strength function of  $^{100}\text{Mo}$  may indicate a large static quadrupole deformation in the ground state. Indeed, in the analysis of the isovector dipole strength, the situation of  $^{100}\text{Mo}$  is also different from the lighter isotopes [7]. In Ref. [8] the issue of pairing correlation and the axial deformation have been discussed.

In this work, we calculate the strength of the ISM vibration mode by constraining the ground state to a few typical deformations. In particular, the TDDFT + BCS code allow for the continuous increase of the triaxial degree of freedom. The resulted strength functions are compared with the experimental data. This approach may allow for a quantitative determination of a static triaxial deformation in the ground state of  $^{100}\text{Mo}$ . In Sec. II we briefly introduce the TDDFT + BCS method and the

\*Electronic address: [yueshi@hit.edu.cn](mailto:yueshi@hit.edu.cn)

†Electronic address: [p.stevenson@surrey.ac.uk](mailto:p.stevenson@surrey.ac.uk)

<sup>1</sup> The coupling constants of an energy density functional (EDF) are usually determined to give reasonable description for the ground-state properties of the double-magic nuclei

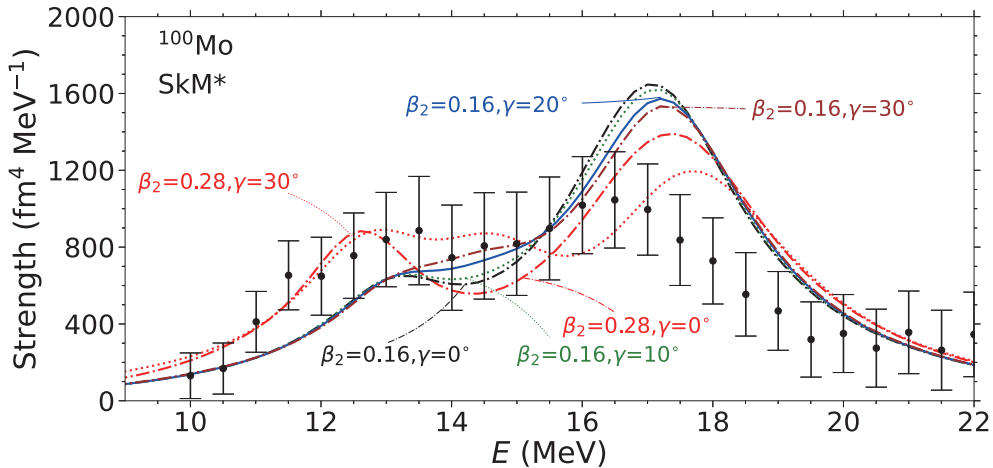


FIG. 1: The ISM strengths calculated using the TDDFT method with the SkM\* EDF. The experimental data are extracted from Refs. [1, 2].

parameters used. Section III presents the results and discussions. Section IV summarizes the current work.

## II. THE MODEL

To study the isoscalar monopole vibration of triaxially deformed nuclei, we perform three-dimensional (3D) symmetry-unrestricted TDDFT calculations [7]. In the static calculations, the functional contains all the time-even and time-odd terms except for the tensor contribution. This is due to the consideration of the local gauge invariance of the energy density. For the pairing treatment, we adopt the Bardeen-Cooper-Schrieffer (BCS) method. In Ref. [7] we applied the same TDDFT + BCS method to describe the isovector dipole resonances in the Zr, Mo, and Ru nuclei. In this work, we use the same pairing strengths for the ground state of  $^{100}\text{Mo}$ .

We choose to use four EDFs, namely the SkM\* [9], SkP [10], UNEDF1 [11], and SLy4 [12] EDFs. The SkM\* and UNEDF1 EDFs are fitted to take into account the properties of deformed nuclei. The SkP EDF has smaller incompressibility parameter  $K_\infty$  and  $m^*/m = 1$ . This makes SkP successful in describing the isoscalar giant monopole resonance in tin isotopes. The SLy4 EDF was fitted to have better performance for the neutron-rich nuclei.

In this work we calculate the ISM strengths with the quadrupole deformations being constrained at a few deformations and compare the calculated strength functions with observed ones. The quadrupole deformation are characterized by the parameters  $\beta_2$  and  $\gamma$  which are related to the quadrupole moments via

$$\beta_2 = \sqrt{\frac{5\pi}{9}} \frac{1}{AR_0^2} \sqrt{Q_{20}^2 + Q_{22}^2},$$

$$\gamma = \arctan(Q_{22}/Q_{20}),$$

where  $A = N + Z$  and  $R_0 = 1.2A^{1/3}$  fm. The quadrupole moments  $Q_{20}$  and  $Q_{22}$  are defined as

$$Q_{20} \equiv \langle \Phi | 2z^2 - x^2 - y^2 | \Phi \rangle,$$

$$Q_{22} \equiv \sqrt{3} \langle \Phi | x^2 - y^2 | \Phi \rangle,$$

where  $|\Phi\rangle$  denotes the mean-field ground state. The constraint calculations similar to those of Ref. [13] are performed to give the desired  $Q_{20}$  and  $Q_{22}$  value.

The ISM vibrational mode is accessed by applying a small instantaneous boost on single-particle wavefunctions

$$\psi_{i,q}(\mathbf{r}, \sigma; t = 0+) \equiv \exp(-i\epsilon r^2) \psi_{i,q}(\mathbf{r}, \sigma), \quad (1)$$

where the typical magnitude of  $|\epsilon|$  is  $10^{-3} \text{ fm}^{-2}$ . The following time-dependent procedure are then performed to obtain the time varying mean-field wavefunction  $|\Phi(t)\rangle$ , as described in Ref. [7]. The expectation value of the isoscalar monopole moment  $D(t) = \langle \Phi(t) | r^2 | \Phi(t) \rangle$  is recorded up to  $1000 \text{ fm}/c$ . The strength function is calculated by performing a Fourier transform of the monopole moment

$$S(E; E0) = -\frac{1}{\pi\hbar\epsilon} \text{Im} \int D(t) e^{(iE - \Gamma/2)t/\hbar} dt, \quad (2)$$

where the smoothing parameter is taken to be  $\Gamma = 2 \text{ MeV}$ . We expand the time propagator in terms of the Taylor series up to the fourth order. The energy-weighted sum rules obtained by integrating the strength functions 2 and those obtained using the ground-state densities [14] are compared. The results agree on the level of a few percentages ( $< 5\%$ ).

## III. RESULTS AND DISCUSSIONS

Figure 1 shows the ISM strengths calculated for a few deformations using the TDDFT + BCS method (SkM\*

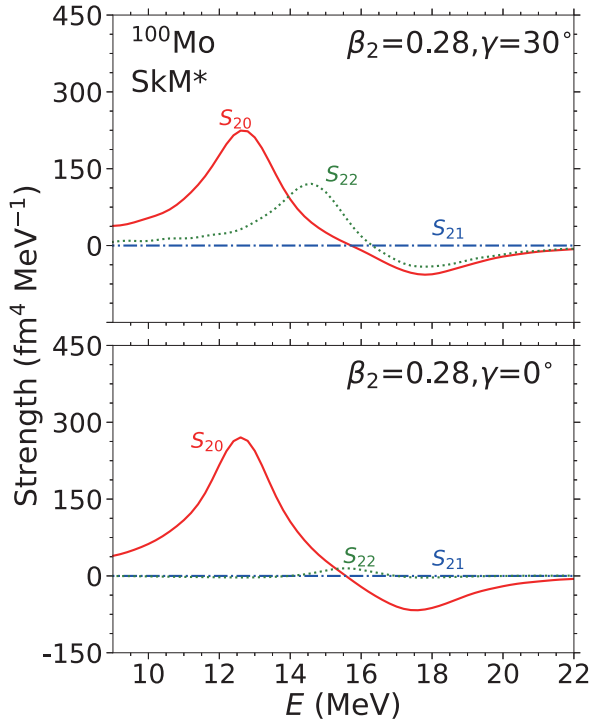


FIG. 2: The strengths corresponding to the response of the  $Q_{20}$  ( $S_{20}$ ),  $Q_{21}$  ( $S_{21}$ ), and  $Q_{22}$  ( $S_{22}$ ) moments.

EDF). For the smaller quadrupole deformations ( $\beta_2 = 0.16$ ), the main peaks at higher energy ( $E \approx 17$  MeV) are much more pronounced than the low-energy peaks. With increasing triaxial deformation  $\gamma$ , the lower-energy peaks for  $\gamma = 0^\circ$  at  $E \approx 13.5$  MeV become less distinguishable and become shoulders at  $\gamma = 30^\circ$ .

For lighter Mo isotopes, the observed ISM strength functions show pronounced giant monopole peaks and shoulders on the lower-energy side [1, 2]. It can be expected that this feature in the lighter isotopes can be reproduced by the calculated strengths based on a smaller deformations ( $\beta_2 \approx 0.16$ ) as shown in Fig. 1.

For a larger  $\beta_2 = 0.28$ , the two peaks become more separate. With  $\gamma = 20^\circ, 30^\circ$ , the low-energy peak separates into two peaks forming a broader plateau joining the peak at higher energy. The main peaks occurring at higher energies  $E \approx 17.5$  MeV are much lower in height compared to those calculated based on a smaller  $\beta_2 = 0.16$ .

In Fig. 1, the calculated strength functions are compared with the experimental data [1, 2]. It can be seen that all the calculations overestimate the energy of the second peak. The observed strength function peaks at  $E \approx 16.5$  MeV. The calculations overestimate the data by  $\approx 0.5$  and  $\approx 1.0$  MeV for  $\beta_2 = 0.16$  and  $\beta_2 = 0.27$ , respectively. This is due to a large incompressibility ( $K_\infty$ ) that the SkM\* EDF predicts,  $K_\infty = 217$  MeV, as noted in Ref. [8].

Nevertheless, for  $(\beta_2, \gamma) = (0.28, 20^\circ/30^\circ)$ , the calculated strengths show features that reproduce the data both in the rising part and the general peak structure.

Compared to the strength functions of a smaller  $\beta_2$  value, those corresponding to larger  $\beta_2$  are more spread and less pronounced. In particular, when the  $\gamma$  value is increased the lower peak becomes a plateau, which becomes closer to the experimental data.

In Ref. [8] the low-energy shoulder has been interpreted as a coupling between the isoscalar monopole and the isoscalar quadrupole vibration mode. A similar two-peak structure has been discussed in the ISM strengths in the Sm isotopes in random-phase approximation calculations based on axial deformations [15]. These studies draw their conclusions from an examination of the isoscalar quadrupole strength functions which peak at similar energy as that of the low-energy peak of the ISM strength function. Here we try to understand the coupling in our TDDFT + BCS calculation [16].

In Fig. 2 we plot the Fourier transform of the relevant quadrupole moments,  $Q_{20,21,22}(t)$ 's after the ISM boost, which corresponds to the solid red curves  $(\beta, \gamma) = (0.28, 0^\circ/30^\circ)$  in Fig. 1. We note that the two quadrupole modes,  $S_{20}$  and  $S_{22}$ , show significant strengths at  $E = 12.5$  and  $14.5$  MeV which are responsible for the first and second peaks in low energy region (see Fig. 1). Whereas the  $S_{21}$  mode shows zero strength meaning there is no coupling between this mode and the ISM mode.

When  $\gamma = 0^\circ$  the coupling between the  $Q_{22}$  mode and the ISM mode is zero. Because for an axially deformed nucleus with the  $z$ -axis being the symmetry axis, the  $Q_{22} \equiv \sqrt{3}\langle x^2 - y^2 \rangle$  value will stay zero when the whole nucleus is expanding or contracting equally in three directions. The same reasoning applies to the  $Q_{21} \propto \langle xz \rangle$  case too. In this case, an  $r^2$  boost will not make the density lose the  $xy$ ,  $xz$ , or  $yz$  plane flip symmetry.

Figure 3 shows the strength functions calculated with the SkP EDF. This EDF has a  $K_\infty = 202$  MeV. In spherical calculations, the single resonance peak is supposed to be lower compared to the spherical SkM\* result. In our deformed calculations, the main peak is delayed but still reproduces the resonance energy at  $E \approx 16.8$  MeV. The energy of the main peak based on results of  $\beta_2 = 0.16$  are lower by  $0.5$  MeV compared to the data. Again, we notice a larger  $\beta_2$  value ( $0.25$ ) together with a triaxial deformation ( $30^\circ$ ) can reproduce the general shape of the observed strength function.

Figure 4 displays the ISM strengths calculated using the UNEDF1 EDF. This parameterization is obtained by taking into account the properties of deformed nuclei. The  $K_\infty = 220$  MeV for UNEDF1 parameterization. Again, it can be seen that the strengths at the lower-energy part can be reproduced by the calculation based on a deformation of  $\beta_2 \approx 0.25, 0.30$ . For the results of  $\beta_2 = 0.25$ , we include  $\gamma = 20^\circ$  and  $30^\circ$ , it is clear that the increase of  $\gamma$  results in the plateaus between the two peaks. The heights of the calculated plateau part for  $E \sim 12 - 14$  MeV are lower compared to other EDFs for UNEDF1. Consequently, this parameter requires a larger  $\beta_2 = 0.3$  value to best reproduce the data.

Figure 5 displays the strengths calculated using the

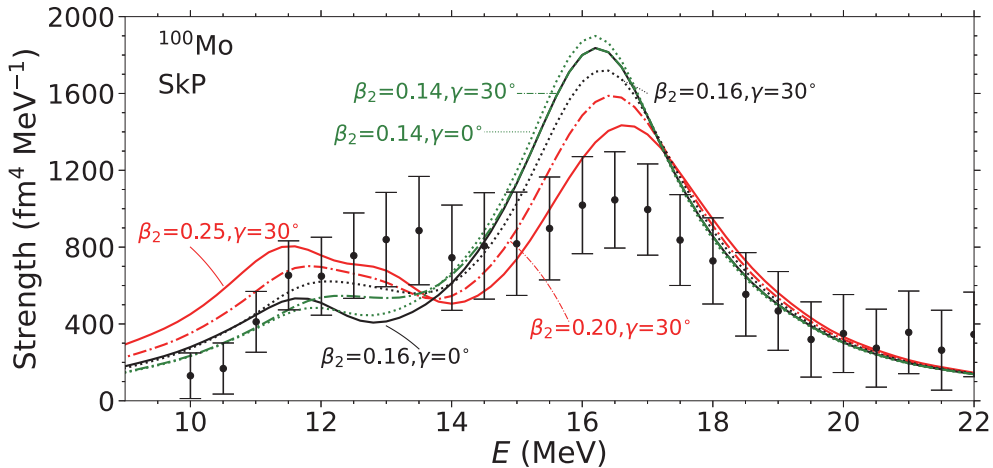


FIG. 3: Similar to Fig. 1, except for SkP EDF.

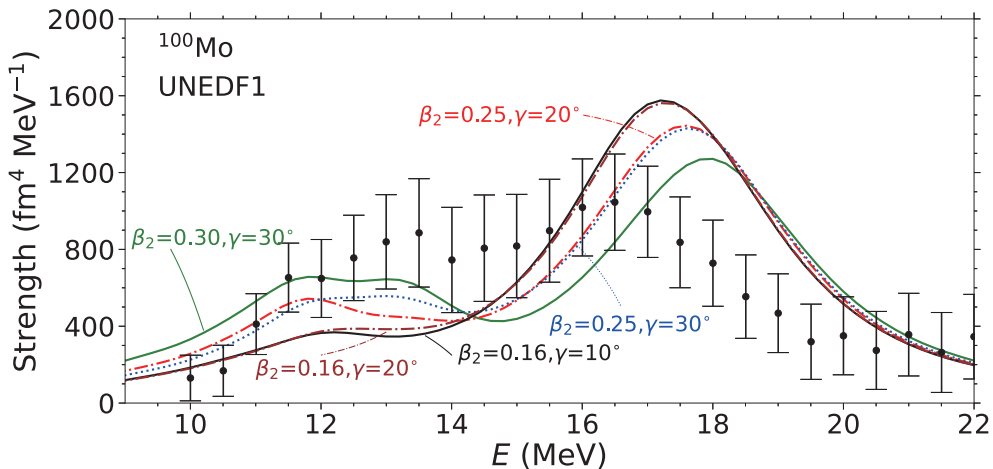


FIG. 4: Similar to Fig. 1, except for UNEDF1 EDF.

SLy4 EDF. For results based on a smaller deformation,  $\beta_2 \approx 0.2$ , similar curves have been seen in the case of the SkM\* EDF. For the strength based on a deformation of  $(\beta_2, \gamma) = (0.28, 30^\circ)$ , we notice a similar agreement with the data as those given by the SkM\* EDF at the same deformation (Fig. 1). However, the higher-energy peak is at  $E \approx 18.2$  MeV, which is  $\sim 1.5$  MeV higher than the observed one. This is due to the large  $K_\infty = 230$  MeV predicted by the SLy4 EDF.

One interesting observation is that all four EDFs predict similar widths for the strength functions at similar deformations. The SkM\*, SLy4, and UNEDF1 EDFs reproduce the energy of the rising part of the observed strength function, but overestimate the second peak, giving a broader general strength peak. The results with SkP EDF underestimate the energy corresponding to the rising part but reproduce the second peak. We note that the FSUGarnet parameter of relativistic mean field theory seems to predict a narrower giant ISM peak in the spherical calculations [2]. It is interesting to see the deformed calculation using this method [17].

#### IV. SUMMARY

In summary, we study the isoscalar monopole (ISM) mode of the strength function in  $^{100}\text{Mo}$  using the symmetry-unrestricted 3D time-dependent density functional theory including a BCS pairing (TDDFT + BCS). Since the shape of the strength function depends on the ground state deformation, we constrain the ground state to a few sampling deformations before the time-dependent study.

The calculated strength functions show two peaks if the axial deformation  $\beta_2$  is in the region of 2.5 – 2.8. Increasing the triaxial parameter  $\gamma$  results in the low-energy peak splitting and forming a plateau area in the low-energy region ( $E \sim 12 - 14$ ). When  $(\beta_2, \gamma) = (0.28, 30^\circ)$ , the calculation reproduces the experimental data. Hence, our microscopic calculations suggest a medium  $\beta_2$  value and a static triaxial deformation in the ground state of  $^{100}\text{Mo}$ .

Our time-dependent study allows for studying the time response of quadrupole moments after an ISM boost.

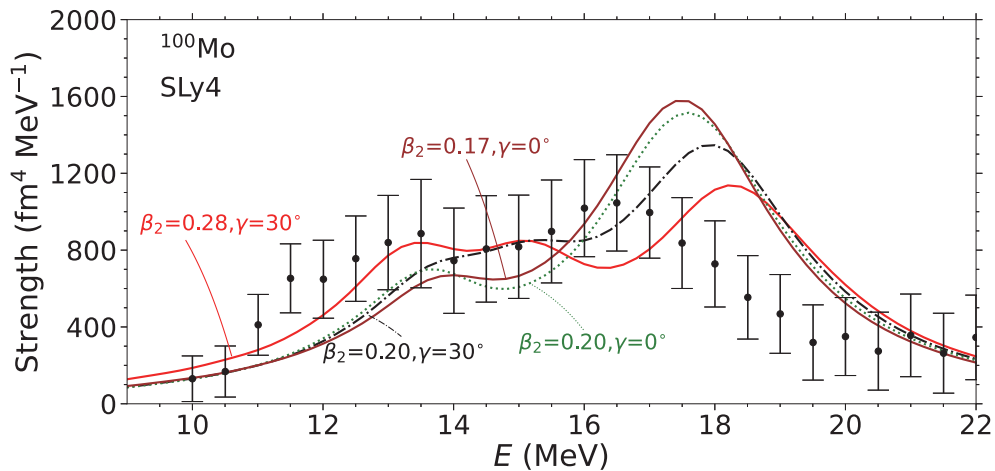


FIG. 5: Similar to Fig. 1, except for SLy4 EDF.

The analyses show that the occurrence of the low-energy peak is due to a coupling of the ISM mode and two isoscalar quadrupole modes ( $K = 0, 2$ ). When the nucleus becomes triaxially deformed, the two quadrupole modes split, resulting in the split of the low-energy peak. This brings the calculation closer to the experimental data.

#### Acknowledgments

The current work is supported by National Natural Science Foundation of China (Grant No. 12075068 and

No. 11705038), the Fundamental Research Funds for the Central Universities (Grant No. HIT.BRET.2021003), YS thanks the HPC Studio at Physics Department of Harbin Institute of Technology for computing resources allocated through INSPUR-HPC@PHY.HIT.

Paul, funding info...

- 
- [1] K. Howard, U. Garg, M. Itoh, H. Akimune, M. Fujiwara, T. Furuno, Y. Gupta, M. Harakeh, K. Inaba, Y. Ishibashi, K. Karasudani, T. Kawabata, A. Kohda, Y. Matsuda, M. Murata, S. Nakamura, J. Okamoto, S. Ota, J. Piekarewicz, A. Sakaue, M. Şenyigit, M. Tsumura, and Y. Yang, *Physics Letters B* **807**, 135608 (2020).
- [2] K. Howard, arXiv:2004.02362v1[nucl-exp], 2020, .
- [3] U. Garg and G. Colò, *Progress in Particle and Nuclear Physics* **101**, 55 (2018).
- [4] L.-G. Cao, H. Sagawa, and G. Colò, *Phys. Rev. C* **86**, 054313 (2012).
- [5] T. Li, U. Garg, Y. Liu, R. Marks, B. K. Nayak, P. V. M. Rao, M. Fujiwara, H. Hashimoto, K. Kawase, K. Nakanishi, S. Okumura, M. Yosoi, M. Itoh, M. Ichikawa, R. Matsuo, T. Terazono, M. Uchida, T. Kawabata, H. Akimune, Y. Iwao, T. Murakami, H. Sakaguchi, S. Terashima, Y. Yasuda, J. Zenihiro, and M. N. Harakeh, *Phys. Rev. Lett.* **99**, 162503 (2007).
- [6] J. Piekarewicz, *Phys. Rev. C* **76**, 031301 (2007).
- [7] Y. Shi, N. Hinohara, and B. Schuetrumpf, *Phys. Rev. C* **102**, 044325 (2020).
- [8] G. Colò, D. Gambacurta, W. Kleinig, J. Kvasil, V. O. Nesterenko, and A. Pastore, *Physics Letters B* **811**, 135940 (2020).
- [9] J. Bartel, P. Quentin, M. Brack, C. Guet, and H.-B. Håkansson, *Nuclear Physics A* **386**, 79 (1982).
- [10] J. Dobaczewski, H. Flocard, and J. Treiner, *Nucl. Phys. A* **422**, 103 (1984).
- [11] M. Kortelainen, J. McDonnell, W. Nazarewicz, P.-G. Reinhard, J. Sarich, N. Schunck, M. V. Stoitsov, and S. M. Wild, *Phys. Rev. C* **85**, 024304 (2012).
- [12] E. Chabanat, P. Bonche, P. Haensel, J. Meyer, and R. Schaeffer, *Nucl. Phys. A* **635**, 231 (1998).
- [13] W. Ryssens, V. Hellemans, M. Bender, and P.-H. Heenen, *Comput. Phys. Commun.* **187**, 175 (2015).
- [14] N. Hinohara, *Phys. Rev. C* **100**, 024310 (2019).
- [15] J. Kvasil, V. O. Nesterenko, A. Repko, D. Bozik, W. Kleinig, and P.-G. Reinhard, *Journal of Physics: Conference Series* **580**, 012053 (2015).
- [16] D. Almeded and P. D. Stevenson, *Journal of Physics G: Nuclear and Particle Physics* **31**, S1819 (2005).
- [17] W.-C. Chen and J. Piekarewicz, *Physics Letters B* **748**, 284 (2015).